Performance of 2D/3D medical image registration using compressed volumetric data

Osama Dorgham and Mark Fisher[a] *

[a] School of Computing Sciences, University of East Anglia, Norwich, NR4 7TJ, UK

Abstract. Digitally Reconstructed Radiographs (DRRs) are used in radiation therapy to confirm patient setup prior to treatment. This is often done manually (interactively) but some radiation therapy treatment manufacturers have automated the process. Modern radiation therapy methods place a greater emphasis on accurate patient alignment and there is a need to reduce the time spent on this activity. Furthermore, recently proposed 'moving aperture' approaches addressing motion artifacts during treatment delivery need 'real-time' registration. When alignment is carried out automatically the approach normally adopted is to solve the so called 2D-3D registration problem. Within the 2D-3D registration framework, a reference X-ray image is compared with DRRs derived from a 'floating' CT volume (CT_{Vol}). Generating DRRs is computationally expensive and this is the major bottleneck in the 2D-3D processing chain. A possible way of solving this problem might lie in reducing the number of internal spaces within the CT_{Vol} using an Octree compression. This paper demonstrates that DRRs derived from Octree compressed CT_{Vol} can be registered with reference images with reasonable accuracy (compared to those from uncompressed CT_{Vol}), even when the number of internal spaces (voxels) are reduced by 90%.

1 Introduction

Radiotherapy represents a fast, accurate and effective way of destroying cancer cells and remains an effective treatment for a large number of patients. One of the benefits of modern Intensity Modulated Radiotherapy Treatment (IMRT) lies in its ability to more accurately target cancerous tissue, however this places a greater emphasis on the need for accurate patient positioning systems. 2D-3D medical image registration is an established approach used register the patients' anatomy with previously acquired volumetric data prior to radiotherapy or surgery. Registration is achieved by comparing reference X-ray images, acquired during surgery or radiotherapy, to template images (Digitally Reconstructed Radiographs (DRRs) derived from volumetric data). The process returns a rigid transformation (rotation and/or translation) which is applied to the so called 'floating' volume to map the template image to the reference image [1]. In radiotherapy, template images (DRRs) are generated from CT (Computed Tomographic) volumetric data which is routinely acquired for treatment planning. DRRs are formed by summing the attenuation of each voxel along known ray paths through the CT volume (CT_{Vol}) [2, 3]. This type of image is extensively used in medical applications and especially in radiotherapy treatment [4]. Unfortunately the generation of DRR images using ray casting, depicted within Figure 1 [5], is computationally expensive and forms a bottleneck in the 2D-3D registration scheme. Thus, the need for more efficient (real-time) image registration has motivated research into other faster algorithms and architectures for DRR generation [6].

Normally, $p \times q$ rays are cast to generate a DRR from a CT_{Vol}; where p and q are determined by the resolution for the solid-state flat panel X-ray detector used to form the image. This study, investigates the effect on registration performance due to using DRRs reconstructed from CT_{Vol} which have been compressed using an Octree. The Octree, and 2D equivalent Quadtree, are lossy compression algorithms which encode the underlying voxel/pixels as tree data structures, where each internal vertex is formed from up to eight or four children respectively. The Quadtree and Octree representations of 2D surfaces and 3D solid objects are well known approaches with applications in image processing, solid modeling and geographic information systems (GIS) [7]. According to the volume decomposition method, there are two main types of Octree representations, known as regular and irregular. A regular Octree volume is decomposed (split) in equally sized internal spaces and a irregular Octree volume will contain different sizes of internal spaces [8]. Our study uses the irregular Octree representation as this approach gives a slightly better compression figure.

An Octree compressed CT_{Vol} comprises internal spaces, each containing voxels which share similar CT numbers. As such, ray casting through a volume represented as an Octree is potentially computationally simpler. However, significant gains result from there being few internal spaces (i.e. high compression) and in this case compression artifacts will be present in the resulting DRRs. This paper investigates the performance of a 2D-3D image registration scheme using CT_{Vols} compressed as an irregular Octree. The paper proceeds as follows: firstly the method used to generate Octree CT_{Vols} is explained and parts of the 2D-3D registration model used for the experiments are introduced. Then the experimental procedure is outlined and results are presented. The paper concludes with a brief discussion and suggestions for further work.

*email:{O.Dorgham,M.Fisher}@uea.ac.uk

2 Method

2.1 CT volume Decomposition

Octree CT_{Vol} decompositions can be pre-computed off-line. A parameter (P), known as the Pivot value ([0-1]) is used to control the splitting process (i.e. $P = 0$ creates the maximum number of decomposed spaces). The Octree algorithm is applied recursively, and starts by considering an internal space equal in size to CT_{Vol}. We compute the difference in intensities between voxel values in the same space and if the difference grater than a Ratio defined as $(R = P * I_{range})$, where I_{range} is the range of (*intensities*) of different anatomical material (intensity could be calculated in HU or in normalized gray scale level), then the space will be split into eight internal spaces, otherwise it will be represented as a one space. This operation is applied recursively for each of the new internal spaces generated within CT_{Vol} until no more children are created. A three dimensional matrix is used to store the decomposed CT_{Vol} and this is subsequently converted into a list containing (X, Y, Z) coordinates, (d) dimension of the cubic space and (I) the attenuation value within the space. Thus, we don't need to store decomposed CT_{Vol} directly as we can rebuild them from the compressed structure. The Octree decomposition is visualised within Figure 1.

Octree volumes will generate similar compression artifacts to those seen in Quadtrees, illustrated in Figure 2. When there are a large number of internal spaces the effect of block artifacts will be insignificant (Figure 2(b)) but when there are fewer, the effects will be visually apparent (e.g. Figure 2(e)). The compression artifacts are less pronounced in DRR images derived from compressed CT_{Vol}; these are of visually acceptable quality even when high levels of compression have been applied to the CT_{Vols} (Figure 3).

2.2 Generation of DRRs

Voxel values in CT volumes are represented by CT number quantified in Hounsfield Units (HU). The attenuation coefficient of the material comprising each voxel can be recovered by [9]:

$$CTnumber = 1000 * [(\mu_i - \mu_w)/\mu_w]$$

where μ_i is the attenuation value of a particular volume element of tissue (voxel) and μ_w is the linear attenuation coefficient of water for the average energy in the CT beam. Most neighbouring voxels within the CT_{Vol} have similar image acquisition parameters [10] and so the Octree is an appropriate technique for decomposing the CT_{Vols} into internal spaces that share common properties. In turn, each ray cast through multiple voxels within the wider space shares the same properties.

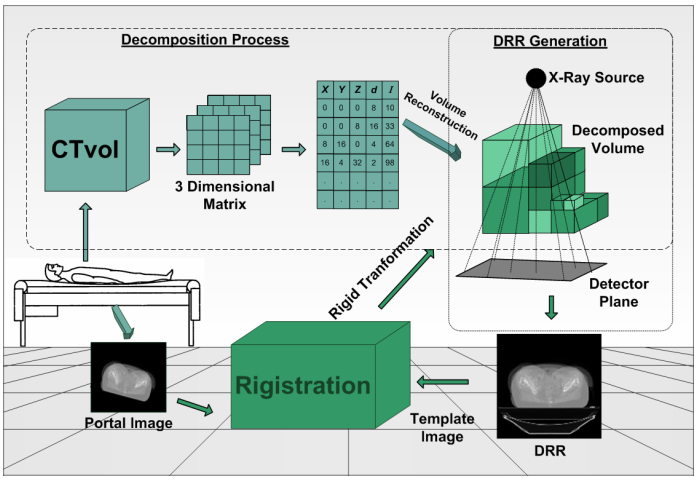

Figure 1. Process workflow

To Generate DDRs we compute the attenuation of a monoenrgetic beam due to different anatomic material (e.g, bone, muscle tissue, epithelial cells, etc.) using Beer's Law [11].

$$I = I_0 * exp^{\Sigma - \mu_i x_i}$$

Where I_0 is the initial X-ray intensity, μ is the linear attenuation coefficient for the voxel (material) through which the ray is cast, x is the length of the X-ray path and subscript i denotes the voxel index along the path of the ray. As this study only addresses the registration performance a conventional ray casting algorithm is used [2]. The development of

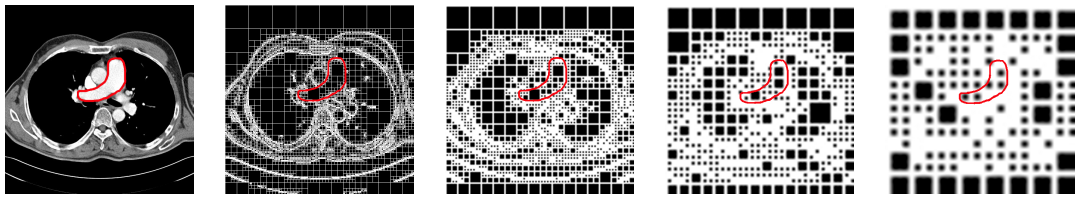

(a) (b) (c) (d) (e)

Figure 2. Illustration of the relation between the size of CT sclice and the size of decomposed spaces. Where (a) shows 512∗512 CT slice before decomposition, (b) 512∗512 decomposed slice, (c) 128∗128 decomposed slice, (d) 64∗64 decomposed slice and (e) 32∗32 decomposed slice.

a new algorithm for generating DRRs will be the focus of future work. X-rays emanate from a point source and strike a flat panel situated behind the patient (i.e. conventional 'C' arm geometry); assumed to be lying on a flat couch. The couch or patient support system (PSS) can be rotated and translated in six degrees of freedom (DOF). The CT volume is quantised in 256*256*133 2 mm^3 voxels, and the flat panel detector models a Varian A500 amorphous silicon detector (ASD) (40 $\times$ 30 cm) operating at an effective resolution of $\tilde{3}$ mm (note: the actual device resolution is a factor of 4 times better but we use low resolution DRRs to reduce computational time). The source and detector are positioned 1.5 m and 1 m from the centre of the CT volume respectively. Example DRR template images from the two CT$_{Vols}$ are shown in Figure 4.

2.3 Registration

Images are compared using normalised cross correlation (Eqn. 1) and an optimisation process adjusts the six parameters (DOF) controlling attitude and position of the PSS (note: other image similarity criteria were explored in a previous paper [12]).

$$CC(I_{ref}, I_j) = \frac{\sum_{i=1}^{N}(A_i - \overline{A}) \cdot (B_i - \overline{B})}{\sqrt{(\sum_{i=1}^{N}(A_i - \overline{A})^2) \cdot (\sum_{i=1}^{N}(B_i - \overline{B})^2)}} \quad (1)$$

where A represents the reference image I_{ref} and B the 'floating' image I_j. N is the total number of image pixels.

To reduce the computational load incurred by repeatedly generating DRR images, arrays of nine DRR images are sequentially computed, each capturing variations in two DOF. The reference image is matched to each of the nine template DRRs and a correlation surface is generated by fitting a 2^{nd} order polynomial. PSS parameters are iteratively optimised until the PSS error between successive iterations reaches zero.

3 Results

Example DRR images reconstructed from Octree CT$_{Vols}$ using a range of P values are shown in Figure 3. Figure 5 illustrates the relationship between P and the compression achieved with respect to a specific (pelvic) CT$_{Vol}$ (in terms of the total number of internal spaces generated).

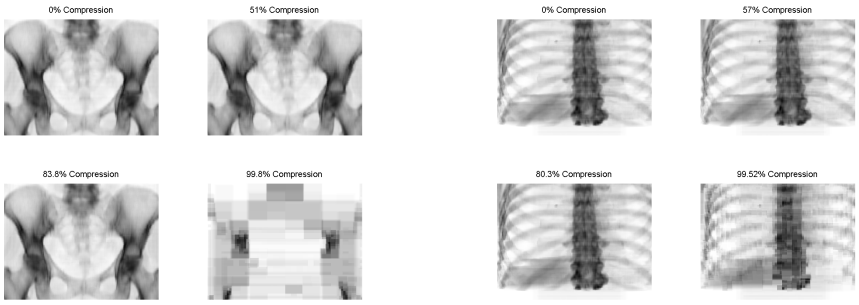

(a) (b)

Figure 3. DRRs derived from compressed CT$_{Vol}$: (a) pelvis; (b) lung

The Octree decomposition process is computationally intensive. Decomposed CT$_{Vol}$ can be generated in O($n^3 \log_8^n$) time, where n represent the size of CT$_{Vol}$. But this is not a concern because they can be precomputed. In this study, DRRs have been computed using a conventional approach which does not exploit the Octree data structure. Each DRR

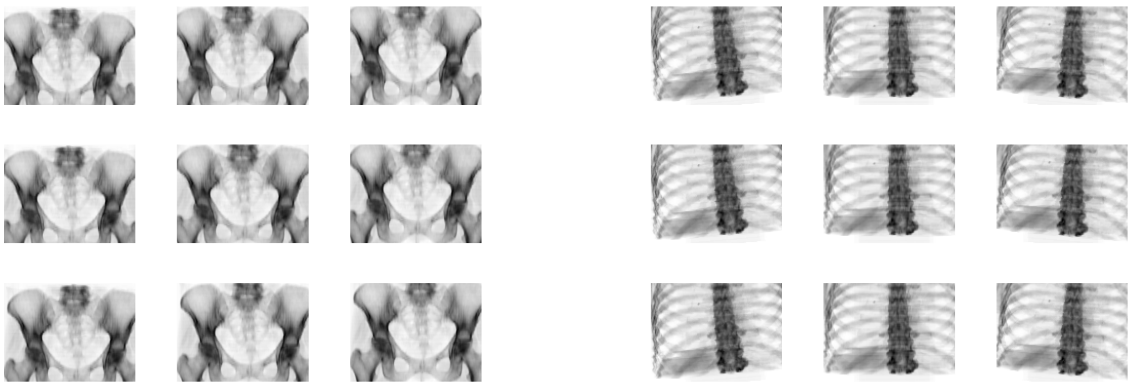

(a) (b)

Figure 4. DRR template image arrays used to build correlation surfaces (each individual DRR image takes 390 ms to reconstruct): (a) pelvis; (b) lung

	CT$_{Vol}$ Size / Compression (%)							
P	32^3		64^3		128^3		256^3	
0	32768	0%	262144	0%	2097152	0%	16777216	0%
0.001	20469	51.37%	149248	47.65%	1097804	43.07%	8159096	37.53%
0.005	18145	68.45%	118903	60.97%	818595	54.64%	5293744	44.63%
0.01	16017	76.60%	100108	69.32%	643455	61.81%	3925720	51.12%
0.015	14904	80.08%	92457	73.75%	550565	64.73%	3342557	54.52%
0.02	14400	83.79%	85800	77.83%	464850	67.27%	2718829	56.05%
0.03	14022	86.06%	80382	80.11%	417075	69.34%	2337959	57.21%
0.04	12874	88.50%	72465	82.93%	358079	72.36%	1929607	60.71%
0.07	9948	91.52%	52592	87.25%	267485	79.94%	1423241	69.64%
0.2	6483	96.68%	35792	93.27%	141051	86.35%	556872	80.22%
0.3	4628	98.51%	25705	95.56%	93073	90.19%	249425	85.88%
0.7	162	99.99%	239	99.98%	377	99.91%	1142	99.51%
1	1	100%	1	100%	1	100%	1	100%

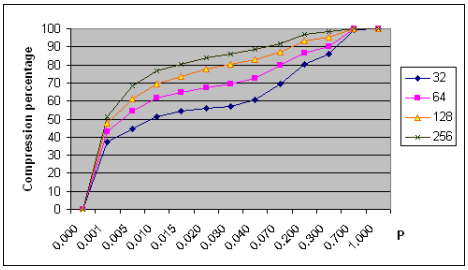

Figure 5. Percentage of compression and total number of internal spaces in pelvic CT$_{Vol}$ at specific P values (Compression value calculated as the reduction in number of spaces relative to the uncompressed spaces number i.e. Volume compression = 1 - (number of internal spaces / total number of voxels).

takes 390 ms. to compute using the conventional approach and a minimum of 27 are needed, so this is a significant factor which limits the usefulness of the approach.

To assess the performance of the registration with respect to compressed CT$_{Vol}$ reference DRR images were generated simulating the ASD at full resolution (512×384). PSS parameters were randomly perturbed in the range ± 10 mm. ± 10 degrees. The 2D-3D registration algorithm was then used to recover the PSS parameters. The experiment was repeated 100 times for a variety of compression levels for both pelvic and lung CT$_{Vol}$. The target registration errors (TRE) are summarised in Figure 6. The tabulated errors can be better understood with reference to the correlation surfaces; an example is illustrated in Figure 7.

	% Compression					
DOF	0%	51%	76%	83.8%	93.1%	99.8%
$\bar{x}$	0.2000 mm	0.2250 mm	0.2400 mm	0.2550 mm	0.2560 mm	2.7390 mm
σ	0.3045 mm	0.3554 mm	0.3823 mm	0.4136 mm	0.4162 mm	1.7823 mm
$\bar{y}$	1.3920 mm	1.7310 mm	1.8260 mm	1.9010 mm	1.8880 mm	8.6250 mm
σ	1.8225 mm	1.9154 mm	2.0550 mm	2.1472 mm	2.2637 mm	10.3380 mm
$\bar{z}$	0.2060 mm	0.6560 mm	0.6720 mm	0.6750 mm	0.6120 mm	2.7240 mm
σ	0.2768 mm	0.3227 mm	0.3502 mm	0.3603 mm	0.3701 mm	3.3388 mm
$\bar{p}$	0.3870°	0.5010°	0.5000°	0.4910°	0.4630°	12.6150°
σ	0.3765°	0.4050°	0.4298°	0.4361°	0.4482°	5.1920°
$\bar{w}$	0.0550°	0.0580°	0.0590°	0.0580°	0.0610°	1.2230°
σ	0.0769°	0.0808°	0.0805°	0.0782°	0.0802°	1.4262°
$\bar{r}$	0.1760°	0.1370°	0.1410°	0.1400°	0.1190°	6.4390°
σ	0.2254°	0.1745°	0.1817°	0.1787°	0.1611°	6.6575°

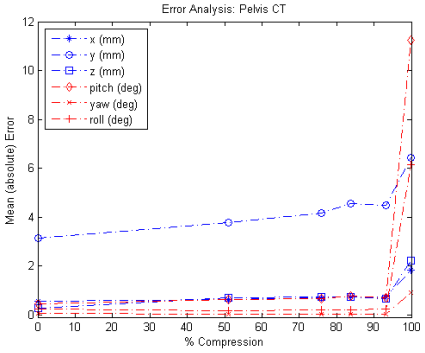

Figure 6. Mean and standard deviation target registration error (TRE) (p = pitch, w = yaw, r = roll).

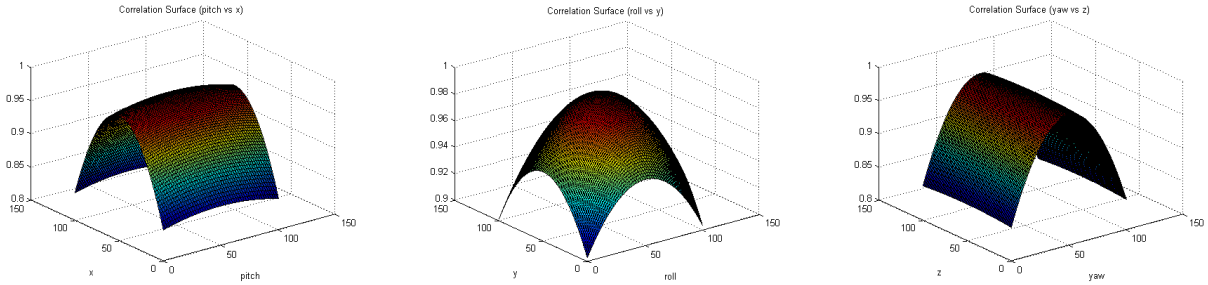

Figure 7. Correlation Surfaces (least squares 2^{nd} order polynomial fit)

4 Conclusions

The results show that 2D-3D registration can recover PSS {x,y,z} translation of up to ± 10 mm. with sub-voxel accuracy (i.e $\ll 2$ mm.) and angular {pitch, yaw, roll} rotations up to ± 10 degrees with an accuracy of better than 1 degree using uncompressed CT_{Vol}. Furthermore, the performance does not degrade significantly when Octree compression is used at levels up to about 95%. The errors in recovered y translations are larger than in x and z since the X-ray fan beam is nearly parallel ($\tilde{4}.5^{\circ}$) and so the geometry is insensitive to adjustments in the height of the couch. In practice, the height of the couch (i.e. patient) much less likely to change compared to x, y translation and p, w, r rotation of the anatomy and so this is not seen as a significant problem. That the 2D-3D registration scheme (0% CT_{Vol}) delivers accurate registrations is not remarkable, but the effect of fitting the polynomial model is noteworthy. We believe this accounts (in some part) for an improvement in TRE over results reported by Khamene *et. al.* [3]. That the performance remains acceptable even at relatively high CT_{Vol} compression rates is much more interesting. In our knowledge this is the first study to demonstrate that compressed volumetric data might be used within a 2D-3D registration framework. Besides the obvious memory saving these data structures afford they appear to offer efficiencies to ray casting approaches, which could be exploited to speed-up the computation of DRR images. This will form a focus for further work.

5 Acknowledgement

This work was partly funded by EU FP6 project No. LSHC-CT-2004-503564, Methods and Advanced Equipment for Simulation and Treatment in Radio-Oncology (MAESTRO). The authors wish to acknowledge their collaboration with the Colney Oncology Centre, Norfolk and Norwich University Hospital and thank them for providing the CT data.

References

1. R. Bansal, L. H. Staib & Z. C. et.al. "A novel approach for the registration of 2D portal and 3D CT images for treatment setup verification in radiotherapy." In *Medical Image Computing and Computer-Assisted Interventation*, pp. 1075–1086. Springer Berlin / Heidelberg, 1998.
2. G. Sherouse, K. Novins, B. Chaney et al. "Computation of digitally reconstructed radiographs for use in radiotherapy treatment design." *Int. J. Radiation Oncology Biol. Phys.* **18(3)**, pp. 651–658, March 1990.
3. A. Khamene, P. Bloch & W. W. et.al. "Automatic registration of portal images and volumetric CT for patient positioning in radiation therapy." *Medical Image Analysis* **10**, pp. 96–112, 2006.
4. J. M. Galvin, C. Sims & G. D. et.al. "The use of digitally reconstructed radiographs for three-dimensional treatment planning and CT-simulation." *International Journal of Radiation Oncology*Biology*Physics* **31**, pp. 935–942, 1995.
5. C. Hurkmans, P. Remeijer & J. L. et.al. "Setup verification using portal imaging; review of current clinical practive." *Radiotherapy and Oncology* **58**, pp. 105–120, 2001.
6. D. B. Russakoff, T. Rohlfing & K. M. et.al. "Fast generation of digitally reconstructed radiographs using attenuation fields with application to 2D-3D image registration." *IEEE Transaction on Medical Imaging* **24**, pp. 1441–1454, 2005.
7. H. Samet. "The quadtree and related hierarchical data structures." *ACM Computing Surveys* **16**, pp. 188–260, 1984.
8. S. R. "Octree-based hexahedral mesh generation." *International Journal of Computational Geometry and Applications* **10**, pp. 383–398, 2000.
9. L. B. Schwartz, D. L. Olive & S. McCarthy. *Diagnostic Imaging for Reproductive Failure*. Taylor and Francis Ltd, UK, 1998.
10. V. R. Preedy & T. J. Peters. *Skeletal Muscle: Pathology, Diagnosis and Management of Disease*. Cambridge University Press, UK, 2002.
11. R. A. Ketcham & W. D. Carlson. "Acquisition, optimization and interpretation of X-ray computed tomographic imagery: applications to the geosciences." *Comput. Geosci.* **27**, pp. 381–400, 2001.
12. M. Fisher & Y. Su. "2-D to 3-D image registration of EPID and CT images for patient setup prior to radiation therapy treatment and evaluation with 4-D CT signal." In *Proc. Medical Image Understanding and Analysis 2007*, pp. 126–130. July 17–18 2007.